Numerical simulation of bending and failure behaviour of *z*-core sandwich panels

D. Zangani*[1], M. Robinson[2], A. G. Gibson[2], L. Torre[3] and J. A. Holmberg[4]

The failure behaviour of fibreglass sandwich panels with structured internal cores (*z*-cored panels) was studied in bending. A finite element model was developed for the simulation of three point bending tests and this has been validated against experimental results. The model was able to predict both the elastic response and, more importantly, the failure behaviour of the structure. It is therefore suitable for use in the optimising the design of *z*-core sandwich panels for transport applications. The same modelling approach was also applied to the structural behaviour of a larger sandwich panel with a metallic insert which was employed in the design of a semitrailer as part of a demonstration of the viability of the technology.

Keywords: Sandwich composites, Structured cores, FE modelling, Failure mechanisms, Transport structures

Introduction

Sandwich panels have been recently introduced in transport applications, for the construction of railway automotive and marine components.[1] Figure 1 shows the type of structured core panel considered in the present study. This will be referred to as a '*z*-core' panel. These structures can be readily manufactured by an integrated liquid composite moulding process (RTM, VARI or VARTM), in which composite ribs are interlocked with the upper and lower skins. This allows excellent bonding between the corrugations and the skins. A further advantage is that the risk of delaminations resulting from an imperfect bond between the core and the skins can be greatly reduced in comparison to standard sandwich structures.

The *z*-core panel is particularly suited for structural and semistructural body components in transport applications.[2] Advantages are the intrinsic lightness and the possibility of incorporating a number of different functions in the same structure. This might include, for instance, acoustic and thermal insulation. There are also parts consolidation advantages compared with alternative forms of constructions such as steel sections or aluminium profiles. Another potential advantage concerns the energy absorption characteristics of this type of composite panel. It has been demonstrated[1] that these structures can show a progressive failure when subjected to quasi-static and impact in-plane loading.

The present paper describes the flexural behaviour of *z*-core panels with added internal polymer foam[3–7] and aims to improve the understanding of flexural failure modes and develop reliable numerical models to support the design of this type of structural element.

Flexural tests

The *z*-core panel design employed in the present study is shown in Fig. 2. The specimens were 300 mm long and 140 mm wide, with a thickness of 30 mm. The internal corrugation was formed from two layers of 1168 g m^{-2} $[0/45/90/45]_s$ non-crimp quadric-axial E-glass mat, placed back to back to produce a symmetric 2·5 mm thick laminate, with the same resin as the skins. The upper and lower skin thickness was 3 mm. The matrix was an acid cured phenolic resin (J2027L supplied by Blagden Chemicals, Sully, UK). The internal panel voids were filled with a phenolic foam (Contratherm C70-130, Alderley Materials, Berkeley, UK). Relevant properties are provided in Table 1. The overall fibre weight fraction in the laminates was 63%, corresponding to a volume fraction 43%. The laminates were considered to be orthotropic since a biaxial reinforcement was employed. The same values were assumed for the longitudinal and transverse moduli.

For a preliminary design of the structure in flexure it is possible to consider the shear force V, to be carried entirely by the core structure, and the bending moment M, by the skins. The values of the maximum skin stress σ_f, and the corrugation web stress σ_c, can be estimated as follows[8]

$$\sigma_f = \frac{M}{d_f(h-d_f)} \quad (1)$$

$$\sigma_c = \frac{V}{\sin\theta \cdot d_c} \quad (2)$$

being d_f and d_c respectively the skin and web thicknesses, and h the panel thickness. Failure of either the skin or the corrugations was considered in terms of tensile failure or structural instability (buckling). The

[1]D'Appolonia SpA, Via S Nazaro, 19, 16145 Genova, Italy
[2]University of Newcastle upon Tyne, School of Mechanical and Systems Engineering, Stephenson Building, Newcastle upon Tyne, NE1 7RU, UK
[3]University of Perugia, Civil and Environmental Engineering Department, Institute of Chemical Technologies, Italy
[4]SICOMP AB, Box 271, SE 941 26 Piteå, Sweden

*Corresponding author, email donato.zangani@dappolonia.it

Published by Maney on behalf of the Institute
Received 21 September 2007; accepted 28 September 2007
DOI 10.1179/174328907X248195

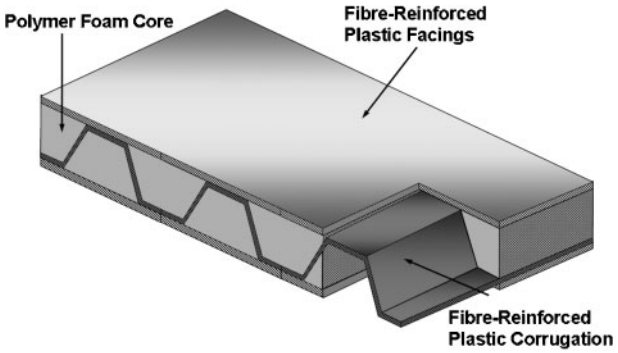

1 *Z*-core sandwich panel with simple corrugation

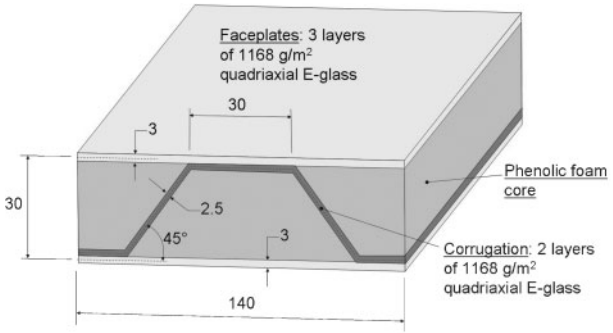

2 Geometry of panel tested in experimental programme, mm

possibility of material compressive failure was ignored as it was considered that this would usually be preceded by buckling. In this simplified analysis the critical stresses are given by[9]

$$\sigma_{f,t} = \sigma_{max,t} \quad \text{(skin failure in tension)} \tag{3}$$

$$\sigma_{f,buckling} = \frac{k_f \pi^2 EI_f}{l_f^2 d_f}$$

(skin instability in compression) (4)

$$\sigma_{c,t} = \sigma_{max,t} \quad \text{(corrugation failure in tension), and} \tag{5}$$

$$\sigma_{c,buckling} = \frac{k_c \pi^2 EI_c}{l_c^2 d_c} \quad \text{(corrugation buckling)} \tag{6}$$

$\sigma_{max,t}$ is the laminate tensile strength. l_f and l_c respectively are the length of the skin and web members. I_f and I_c are the second moments of area per unit width for the skin and core member respectively. E is the Young modulus of the composite material in the key orthotropic directions, k_f and k_c are the buckling coefficients

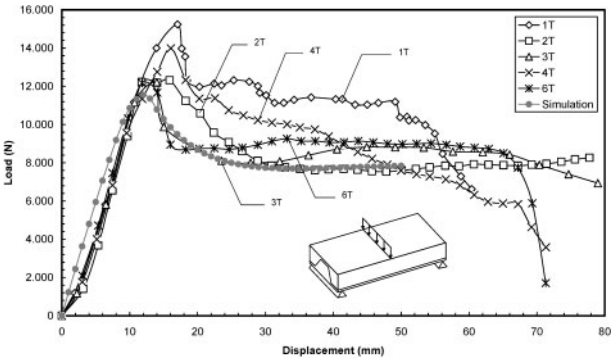

3 Three-point bending tests: load–deflection curve of *z*-core sandwich panels (A configuration)

which are provided by the following expressions[8]

$$k_f = \left(\frac{2{\cdot}4 \cos\theta (d_c/d_f)^3 + 1}{1{\cdot}2 \cos\theta (d_c/d_f)^3 + 1} \right)^2 \tag{7}$$

$$k_c = 1{\cdot}375 \left(\frac{2{\cdot}2 + 1{\cdot}2 (d_f/d_c)^3 \Big/ \cos\theta}{1{\cdot}6 + 0{\cdot}6 (d_f/d_c)^3 \Big/ \cos\theta} \right) \tag{8}$$

The above equations can be used to calculate a good preliminary estimate of the critical loads for failure of the panel components.

In order to improve on the assumptions of the simple model, and to take into account of the foam contribution, a finite element model was used, in conjunction with experimental tests performed at the University of Perugia using ASTM C 393-94. All test specimens had a width of 140 mm and length of 300 mm. Although these dimensions are relatively large, this ensured that the samples were wide enough to contain a representative section of the internal structure. To assess possible effects in panel performance associated with the structural asymmetry of the single corrugation, tests were conducted with the panel samples in both possible orientations. 'A' refers to the panel with the narrow side of the corrugation upwards, as shown in Fig. 2. 'B' refers to the inverted version of this. Figure 3 shows the load–deflection curves of five panels in the 'A' configuration and Fig. 4 the equivalent results for the 'B' configuration. It can be seen that although the measured values of maximum load were fairly similar in both cases, the shape of the curves around the region of the maximum load is a little different in the two configurations. The peak in configuration 'B' appeared to be a little sharper, suggesting the possibility of failure due to instability in this case.

Table 1 Main material properties

	Small scale sandwich panels		Full scale structure	
Property	C70-130 foam	Laminates	Divinycell foam H60	Laminates
Density, kg m^{-3}	130	1800	60	2040
Longitudinal Young's modulus, GPa	0·117–0·135	15·4	0·060	14·0
In plane shear modulus, GPa	n.a.	5·50	n.a.	3·70
Poisson's ratio	0·25–0·44	0·16	0·3	0·28
Compression strength, MPa	0·87–0·95	218	0·80	n.a.
Tensile strength MPa	n.a.	198	1·6	170

n.a., not available.

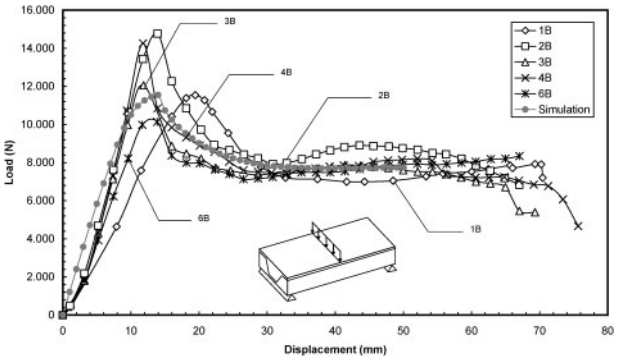

4 Three-point bending tests: load–deflection curve of *z*-core sandwich panels (B configuration)

Finite element (FE) simulation of flexural tests

Figure 5 shows the finite element model used to simulate the bending tests. The ANSYS package was used. The model has a length of 300 mm, a width of 140 mm and a thickness of 32 mm. Because of symmetry, only a quarter of the panel was modelled. The model permits simulation of both the A and B configurations. Volume elements were chosen for both the composite and the foam. Shell elements were initially considered, but rejected mainly because of the difficulty of accurately modelling the geometry of the contact region between the skins and the corrugation. There were also problems with the three dimensional nature of the local stresses around the loading points. Layered eight-node solid elements from the ANSYS library were used for the laminate, with three degrees of freedom at each node. Three layers of volume elements each were used for the upper and lower skin, and two were used for the corrugation. This corresponded to the number of layers of multi-axial fabric in each of these components.

The composite material was considered linear elastic up to failure, which was assumed to be controlled by the maximum stress criterion

$$\frac{\sigma_{x,t}}{\sigma^{f}_{x,t}} \geqslant 1 \quad or \quad \frac{\sigma_{x,c}}{\sigma^{f}_{x,c}} \geqslant 1$$

fibre failure in tension and compression

$$\frac{\sigma_{y,t}}{\sigma^{f}_{y,t}} \geqslant 1 \quad or \quad \frac{\sigma_{y,c}}{\sigma^{f}_{y,c}} \geqslant 1$$

matrix failure in tension and compression (9)

$$\frac{|\sigma_{xy}|}{\sigma^{f}_{xy}} \geqslant 1 \quad \text{shear failure}$$

where σ_x represents the stress in the x direction and $\sigma^{f}_{x,t}$ represents the failure stress in tension. This criterion was implemented into a user subroutine, which was launched at each iteration, corresponding to each increment in applied displacement, which was applied in 1 mm increments. When failure was detected, the appropriate stiffness properties of the ply were set to zero depending on the failure mode. The composite material has been modelled using a linear total stress–total strain curve, starting at the origin, with positive stress and strain values, with slope corresponding to the elastic modulus of the material. The foam was modelled as an isotropic material with plasticity law defined on the basis of experimental data from compression tests.

5 Finite element model of *z*-core panel for simulation of three-point bending tests (one-fourth of panel is modelled for symmetry)

The results of the FE bending simulation are shown in Figs. 3 and 4 alongside the experimental curves for the configuration A and B respectively. Generally good agreement can be observed. The FE simulations confirmed the earlier hypothesis that the failure of the structure was due to instability of the internal webs of the corrugation. Figure 6 shows the displacements in the structure corresponding to an applied displacement of $\sim$15·8 mm in the A configuration. The web of the corrugation has started buckling towards the external side of the panel. The different behaviour between the A and B configurations is shown in Fig. 7. Here the elements of the foam have been removed to allow easier visualisation of the deformation of the structure. The A configuration was characterised by instability of the webs of the corrugation, which buckle outwards, toward the external side of the panel, compressing the foam in the lateral upper part of the sandwich. The instability of the webs in the B configuration was towards the inner part of the sandwich, corresponding to compression of the foam between the two webs of the corrugation.

The failure behaviour of the sandwich panel under flexure was therefore governed by the stiffness of both the webs of the corrugation and of the foam, which provided an effective constraint to buckling.

Analysis of large panel with insert

The structural concept of the *z*-core panel described previously was applied to the manufacture of a full scale structure representative of a structural floor panel for a transportation vehicle. The reference application was the structure of the floor of a semitrailer, including the design of the connection with the metallic substructure. The floor was designed as a sandwich structure with an internal corrugation and a metallic insert inside the corrugation. The design, as shown in Fig. 8, was an extension of the concept in the A configuration described above, with the introduction of the insert at the bottom of the internal corrugation. The purpose of this was to avoid instability of the sandwich components; to reinforce the structure in the load bearing area; and to distribute the forces from the wheels over a wider

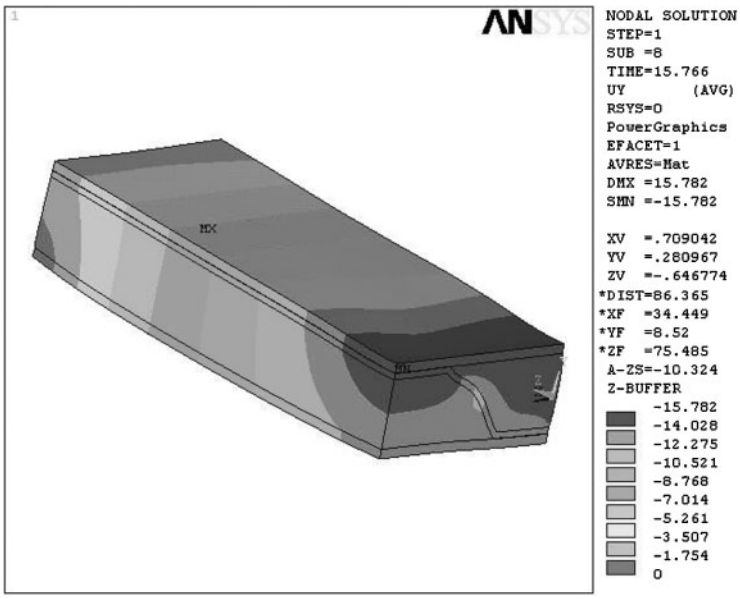

6 Distribution of displacements in panel bending analysis: imposed displacement of 20 mm distribution of total displacements, mm

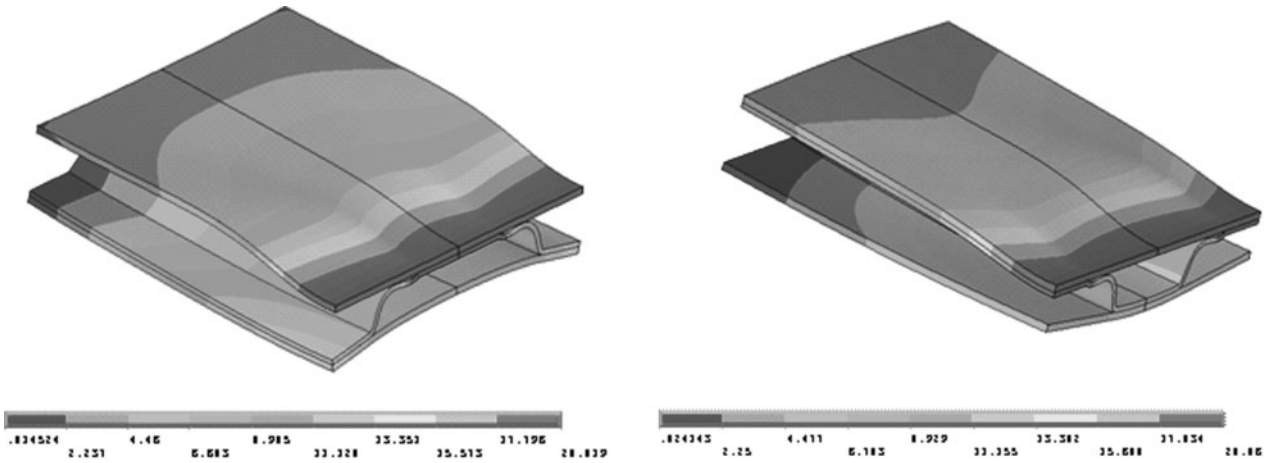

7 Deformation of composite layers in panel during bending test, A configuration (left) and B configuration (right

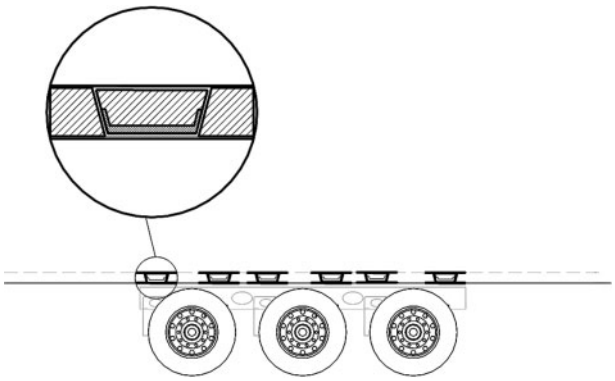

8 Sketch of design concept for structural floor of semi-trailer with corrugated core and metallic inserts for connection of composite floor to underframe

area. Reference loading conditions are depicted in Fig. 9. These correspond to a full scale flexural test where the load from the running wheels was applied to the insert in the middle of the corrugation. For the test was designed to verify the pull-out resistance of the metallic insert under relevant loading conditions. The

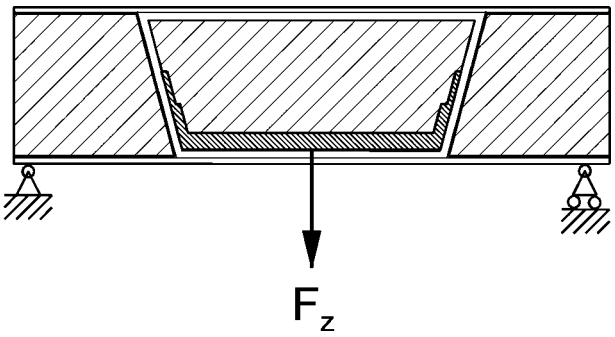

9 Schematic of three-point flexural test

test set-up is depicted in Fig. 10 with indication of the main dimensions. The panel had dimensions of 800 mm length, 800 mm width and 130 mm thickness. The composite lay-up was manufactured by a combination of layers comprising unsaturated polyester resin and biaxial non crimp E-glass fabric (1700 g m^{-2}), thickness, 1·3 mm, with plain weave E-glass fabric (600 g m^{-2}), thickness, 0·45 mm. The core material in this case was cross-linked PVC foam, density 60 kg m^{-3}.

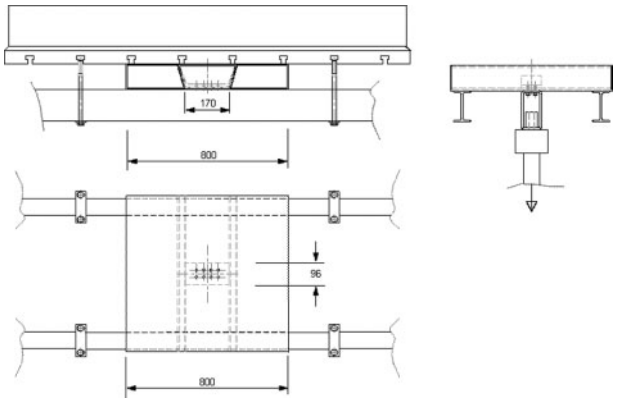

10 Schematic of test condition corresponding to composite panel (800 × 800 mm) supported by two metallic I beams transversal to corrugation direction and with insert at centre

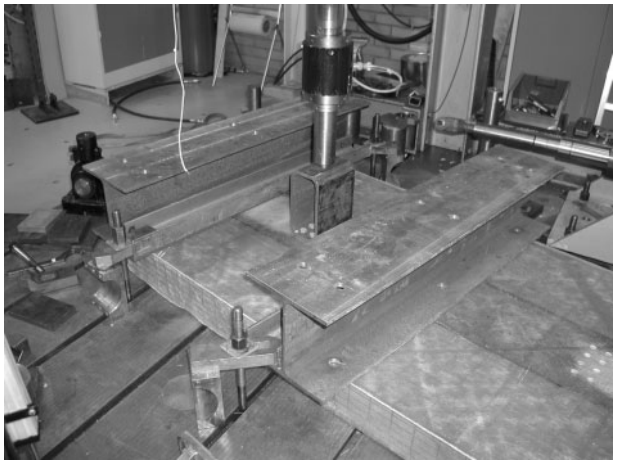

11 Test section mounted in test rig for flexural test

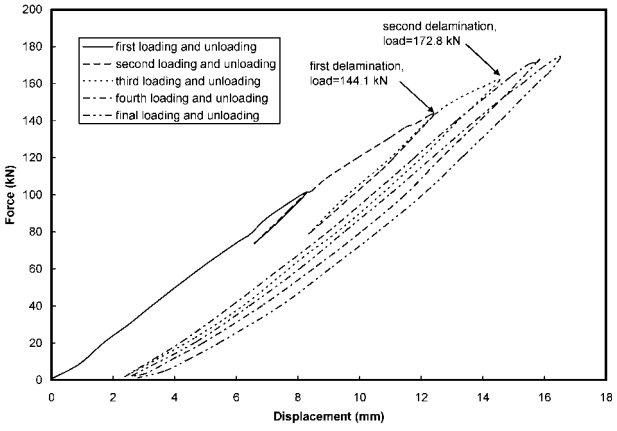

12 Flexural test on first prototype of composite floor with five loading and unloading cycles: first delamination occurring in correspondence of joint at ~144 kN of loading; second delamination at ~172·8 kN

Two large scale flexural tests were performed at SICOMP. The test rig with the sample mounted for the test is shown in Fig. 11. The results of the two tests are shown in Figs. 12 and 13. The curves show almost linear behaviour up to the point of first delamination, which was observed in the composite layer around the insert at a load of ~145 kN. Increasing the load, a larger

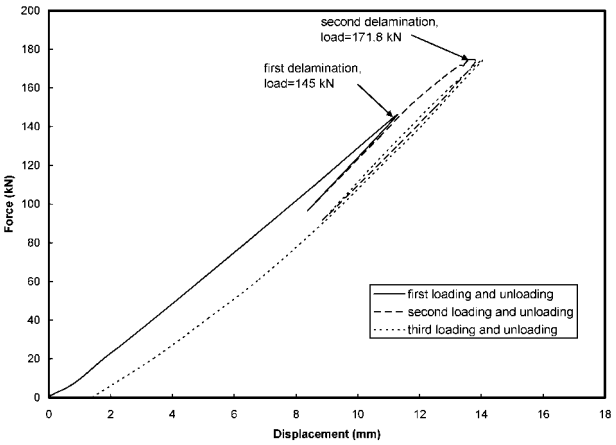

13 Results of flexural test on second prototype of composite floor, with first delamination occurring at 145 kN of loading and second delamination at 171·8 kN

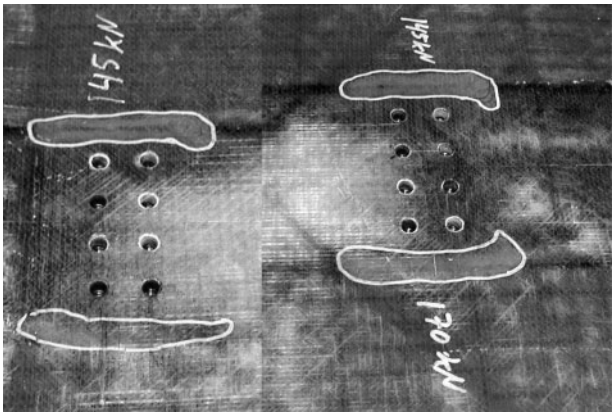

14 Details of extension of delaminations at surface of composite floor in correspondence to insert position

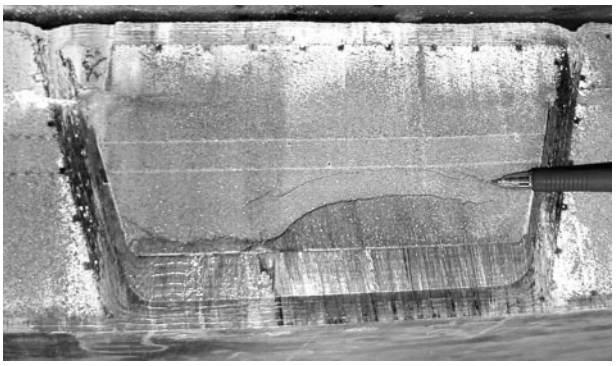

15 Section of sample after testing showing failure of foam above metallic insert

delamination was observed, at a value of ~170 MPa. Figure 14 shows a detailed area indicating the extent of the delaminations, which were localised in the region around the insert and below the webs of the corrugation. A load concentration was expected in this region. A view of the section of the sample after testing is shown in Fig. 15.

The FE model for the flexural test of the composite floor is shown in Fig. 16. Only a quarter of the structure was modelled due to symmetry. A simple support condition was imposed 120 mm from the free edge of

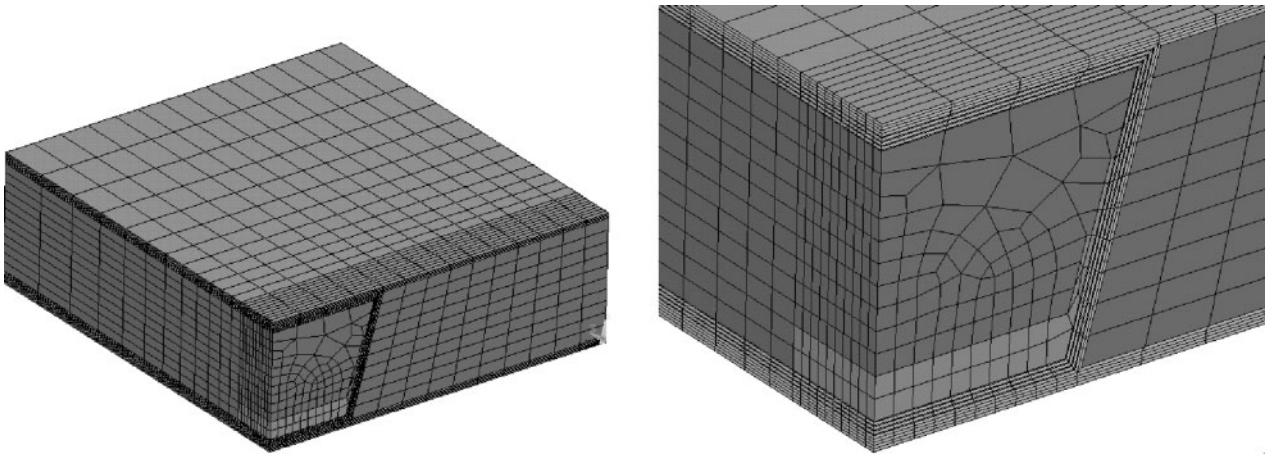

16 Finite element model of joint with rectangular insert and detailed view

the panel. The model used a mapped mesh of layered volume elements for the composite layers and volume elements for the foam and the metallic insert. Higher mesh refinement was used in the region around the insert. A mapped mesh was used to model the composite laminates, in order to better control the direction of the material direction angle for each layer in the laminate. Also, for the foam, both inside and outside the composite beam it was possible to use a mapped mesh of hexahedral elements which had the advantages of maintaining the number of elements at a reasonable level and providing improved analysis efficiency compared with a free mesh of tetrahedral elements. Once again, incremental vertical displacements were applied, in the upper area of the insert. The same material models and failure criteria were used here as were employed in the FE simulation of the small panel flexure test.

Figure 17 shows the comparison between the experimental curves (loading portions) and the FE prediction. The non-linear behaviour of the foam, implemented in the model, was found to be responsible for the non-linear overall response of the model up to $\sim$150 MPa, when the delamination was predicted in the model corresponding to a decrease in stiffness.The areas in the model where delamination occurred are highlighted in Fig. 18. The extent and position of the delaminations are in agreement with the experimental observations. Figure 19 shows the FE predictions of displacement corresponding to an applied displacement of 13 mm above the insert. As expected the higher vertical displacements were localised in the region around the insert in the middle section. The area of higher stress was located below the insert, as shown in Fig. 20. The equivalent stress distribution in the foam is shown in Fig. 21. In this case the model does not predict the failure of the foam above the insert, as shown in Fig. 15. The results show the areas of yield and failure of the foam located near the edges of the insert between the supports. However it was not possible to perform a non destructive assessment of the condition of the foam inside the beam. The FE model would ideally be used in further optimisation of the structure for the industrial exploitation of the concept.

Conclusions

Finite element models for *z*-core sandwich panels have been developed and validated for the assessment of the behaviour of the *z*-core sandwich concept. In bending applications of the *z*-core sandwich concept it is convenient to take advantage of the orthotropic characteristics of the panel to orient the corrugation along the direction of the maximum bending load, to take advantage of the thickening of the upper and lower skins of the sandwich in contact with the corrugation.

The contribution of the foam to the overall response mainly consists of acting as a further link between the upper and lower skins, which partially restricts the tendency of the corrugation to buckle.

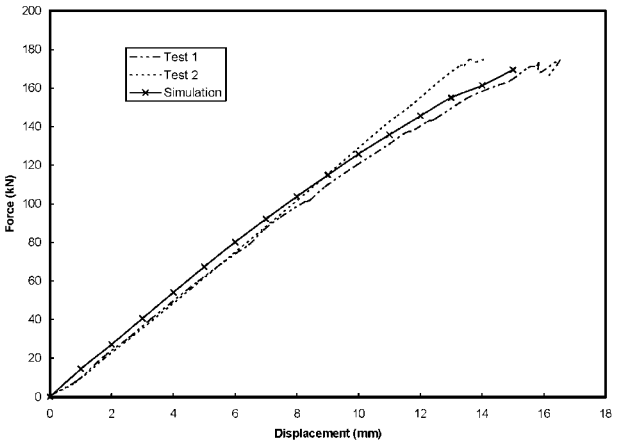

17 Results of simulation of flexural test and comparison with experimental curves

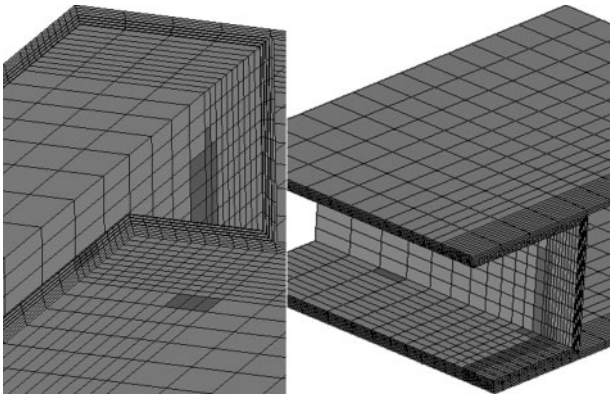

18 Localisation of areas of possible failure due to delamination

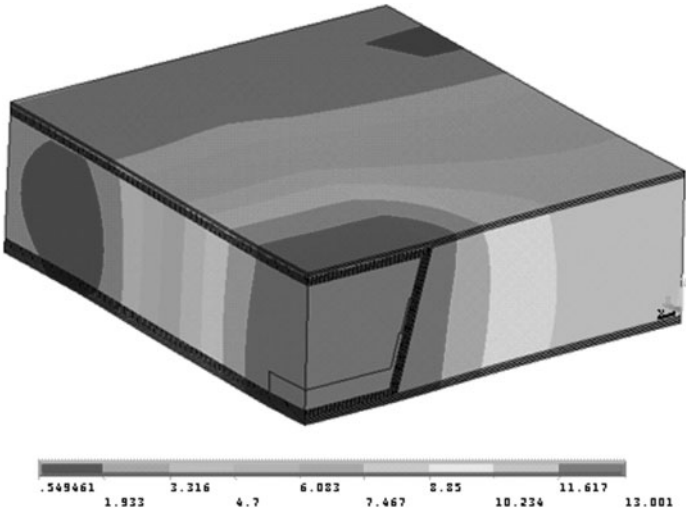

19 Sum of displacements corresponding to 13 mm of applied displacement, mm

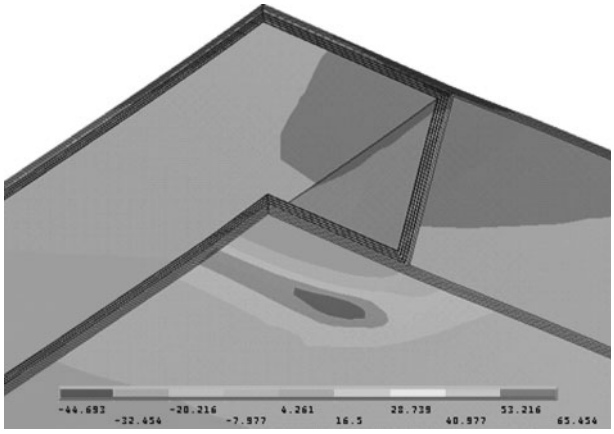

20 Distribution of longitudinal stress (along corrugation), MPa

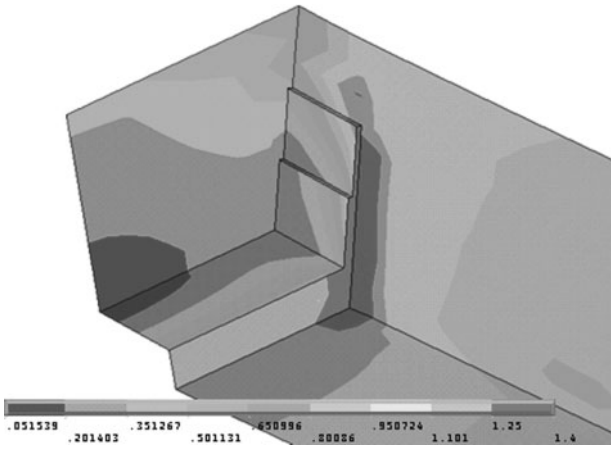

21 Equivalent stress distribution in foam around insert corresponding to 15 mm of applied displacement, MPa

The FEA correlated reasonably well with the experimental measurements and enabled the failure mechanisms to be confirmed. These were due to web buckling in the case of the small scale test samples and delamination in the case of the semitrailer floor.

The numerical results demonstrate that the concept of *z*-core sandwich panel can be very efficient in structural applications, provided that its behaviour can be reliably predicted and the structure can be designed as to avoid instabilities and stress concentrations.

Acknowledgements

This work has been supported by the European Commission and developed under the framework of the GROWTH Project 'Hybrid Composite Production for the Transportation Sector, HYCOPROD', Contract Number G3RD-CT-1999-00060. The authors are grateful to the support received by the other project partners, and in particular to Tord Gustafsson of APC Composit and Kjell Larsson of BoxModul for the support to the design and manufacturing of the composite structures tested in the study.

References

1. M. Robinson: in 'Comprehensive composite materials', Vol. 6, 6.20.1–34; 2000, New York, Elsevier.
2. D. Zangani, A. Barbagelata, O. Manni and G. Mastrobuono: Proc. 2nd Int. Conf. on 'Composites in the rail industry', Birmingham, UK, October 1999, Railview Ltd.
3. T. C. Fung, K. H. Tan and T. S. Lok: *J. Struct. Eng.*, 1994, **120**, (10), 3046–3065.
4. T. C. Fung, K. H. Tan and T. S. Lok: *J. Struct. Eng.*, 1996, **122**, (8), 958.
5. K. H. Ha: Proc. 1st Int. Conf. on 'Sandwich construction', 69–84; 1991, Stockholm, EMAS.
6. T.-S. Lok and Q.-H. Cheng: *J. Struct. Eng.*, 2000, **126**, (5), 552–559.
7. T. M. Nordstrand and L. A. Carlsson: *Compos. Struct*. 1997, **37**, 145–153.
8. H. G. Allen: 'Analysis and design of structural sandwich panels'; 1969, Oxford, Pergamon Press.
9. L. Valdevit, J. W. Hutchinson and A. G. Evans: *Int. J. Solids Struct.*, 2004, **41**, 5105–5124.